Journal of Chromatography, 595 (1992) 221–236
Elsevier Science Publishers B.V., Amsterdam

CHROM. 23 876

Van Deemter-type relationship for determining the optimum initial flow-rate and optimum pressure programming rate in temperature/pressure-programmed capillary column gas chromatography utilizing separation numbers

Louis A. Jones*, William H. Reiss☆ and John J. Glennon

Department of Chemistry, Box 8204, North Carolina State University, Raleigh, NC 27695-8204 (USA)

Thomas M. Gerig

Department of Statistics, Box 8203, North Carolina State University, Raleigh, NC 27695-8203 (USA)

(Received August 20th, 1991)

ABSTRACT

Accurate prediction of the optimum conditions for a double-programmed gas chromatographic separation (simultaneous temperature and pressure programming) has been accomplished for the first time using a new relationship analogous to that established by the Van Deemter equation. Separation numbers (*TZ* values) for $\overline{CH}$, the homologous pair average [*e.g.*, $(C_{12} + C_{13})/2 = C_{12.5}$], were determined for a C_{12}–C_{17} series of *n*-alkanes and related to the average of the elution flow-rate, F_e, of the two homologues used to calculate *TZ*. F_e is defined as the flow-rate at the time of solute elution. Conditions for analysis involved the selection of a low temperature programming rate (*TPR*) and four different initial flow-rates (0.677, 1.10, 1.49 and 1.89 ml/min) upon which was superimposed a series of positive and negative pressure programming rates, *PPr*. Graphs of *TZ versus* F_e were parabolic curves which could be described in terms of longitudinal diffusion and resistance to mass transfer. Higher F_es of 1.49 and 1.89 ml/min resulted in straight lines with negative slopes as only resistance to mass transfer was operating. This effect is discussed in terms of laminar and turbulent flow (as predicted by Reynold's number, *Re*). All plots could be modeled by the quadratic expression $TZ = x(F_e)^2 + y(F_e) + z$. By differentiation, the optimum F_e and maximum *TZ* for each $\overline{CH}$ was determined, and, from this, the optimum initial flow-rate and *PPR* could be derived. The example cited is for the data obtained using an initial flow-rate of 0.677 ml/min, a *TPR* of 0.90°C/min starting at 40°C and nine different *PPR*s. The optimum initial flow-rate determined under these conditions was found to be 0.80 ml/min with an optimum *PPR* of 0.12 kPa/min.

INTRODUCTION

To optimize gas chromatographic (GC) analysis, parameters to be controlled include the column, column length, the coating thickness, the column head pressure (carrier gas velocity) and the oven temperature. The efficiency of a column is related to the amount of band broadening that occurs as the solute traverses the column at a particular column (oven) temperature and carrier gas velocity or flow-rate. In practice, column efficiency is expressed in terms of the height equivalent to a theoretical plate (HETP or *h*) under isothermal conditions as determined by the equation

$$h = \frac{L}{5.54}\left(\frac{w_{0.5}}{t_r}\right)^2 \quad (1)$$

☆ Present address: First Brands Corp., 55 Federal Road, Danbury, CT 06810, USA.

0021-9673/92/$05.00

where L is the length of the column, $w_{0.5}$ is the peak width at half-height, and t_r is the retention time of a solute [1].

The Van Deemter equation [2], originally developed for packed columns, reduces to the well known Golay equation when applied to capillary or open-tubular columns [3]:

$$h = \frac{B}{\mu} + C\mu \tag{2}$$

where μ is the linear flow velocity, B relates to molecular diffusion and C reflects the resistance to mass transfer. The optimum flow-rate or velocity (F_{opt} or μ_{opt}), being that producing the minimum h value (h_{min}) for a selected solute under isothermal conditions, can be determined by plotting flow-rate *versus* h. The minimum h and the corresponding flow-rate or velocity can be visually estimated or, alternatively, eqn. 2 can be differentiated, the term $dh/d\mu$ equated to zero and the optimum flow-rate or velocity determined [4] from the equation

$$\mu_{opt} = (B/C)^{\frac{1}{2}} \tag{3}$$

and the minimum value of h from the following equation (obtained from the substitution of eqn. 3 into eqn. 2):

$$h_{min} = 2(BC)^{\frac{1}{2}} \tag{4}$$

In isothermal GC, the boiling points of homologous solutes and their retention times (t_r), are logarithmically related and higher boiling solutes produce large t_rs and peak widths. In a sample of relatively narrow boiling point range, the chromatogram is characterized by poor separation of early-eluting peaks (narrow peak widths) and broad late-eluting peaks. As a solution to this problem, temperature-programmed gas chromatography (TPGC) has become the most widely used separation technique in GC [5].

Under TPGC conditions, peak widths and retention times can be manipulated by the rate of oven temperature increase, or temperature programming rate (*TPR*), and the Van Deemter relationship no longer applies. An equation which describes the TPGC effect on the resolution between two homologues (a and b) differing by one CH_2 group is the separation number or TZ value [6,7], as described by the equation

$$TZ = \frac{t_r^b - t_r^a}{w_{0.5}^a + w_{0.5}^b} - 1 \tag{5}$$

where $w_{0.5}$ is the peak width at half-height and t_r the retention time for homologues a and b. The quantity TZ is considered to be a measure of the number of peaks separated by 4.7σ resolution that can be placed between two consecutive homologue peaks [8].

Some controversy has been associated with the use of separation number. Rooney and Hartigan [9], in their study of the dependence of TZ on isothermal column temperature, related TZ, N_{eff} (effective plates) and α by

$$TZ = 0.425\left(\frac{\alpha - 1}{\alpha + 1}\right) N_{eff}^{\frac{1}{2}} - 1 \tag{6}$$

and concluded that the increase in TZ with a decrease in column temperature is the result of the increase in α with decreasing temperature. In a study of the dependence of TZ on the rate of column heating in TPGC, Jennings and Adam [10] found that increasing the *TPR* resulted in lower TZ values of the C_{13}–C_{14} homologue pair at both high (33 cm/s) and low (20 cm/s) velocities, the latter providing the higher TZ values. Krupcik *et al.* [11] view the separation number of a column as a "rubber ruler whose length is a function of temperature and is a function not only of the effective plate number which varies with retention as measured by the capacity factor k', but also the relative retention of the *n*-alkanes used ...". However, because of the applicability of TZ values to TPGC, Grob *et al.* [12,13] included the TZ determination as part of their standardized tests recommended for capillary columns.

We have recently completed an in-depth study of h and the TZ values of the homologue pair C_{11}–C_{12} under isothermal column temperature conditions of 40, 60 and 80°C [14]. Coefficients for eqn. 2 were determined, as were the coefficients for an analogous relationship between TZ and linear velocity which had been derived:

$$TZ = A - \frac{B}{\mu} - C\mu \tag{7}$$

Eqns. 2 and 7 were differentiated and determination of the optimum linear velocity (μ_{opt}) needed to provide the minimum value of h (h_{min}) for C_{11} and

C_{12} was carried out. The μ_{opt} required for TZ_{max} was found to be the average of the C_{11} and C_{12} optimum linear velocities, consistant with previous work [15] which had shown that the t_r of TZ was the average t_r of the two homologues.

Plots of h and TZ *versus* flow-rate or linear velocity for each temperature suggested an inverse relationship between these two chromatographic measures of column efficiency, and by substituting the equivalence of $w_{0.5}$ derived from eqn. 1 in eqn. 5, the following equation was obtained:

$$TZ = \left(\frac{L}{5.54}\right)^{\frac{1}{2}}\left[\frac{t_r^b - t_r^a}{(h_a)^{\frac{1}{2}}t_r^a + (h_b)^{\frac{1}{2}}t_r^b}\right] - 1 \qquad (8)$$

where L (mm) is the capillary column length and h_a and h_b are the heights equivalent to a theoretical plate for the homologues a and b. TZ values resulting from triplicate determinations using eqns. 5 and 8 were identical or nearly identical and, when the data of Ettre [8] and Krupcik *et al.* [11] were analyzed, similar excellent agreement was obtained, reaffirming the inverse relationship between TZ and h.

The changes in TZ values of a series of homologues as a function of carbon number with varying TPRs and flow-rates has been investigated [15]. Using three different constant head pressure flows (isobaric) and four different TPRs, it was shown that TZ was related to the average carbon number for a homologous pair by the equation

$$TZ = a(\overline{CH}) + b \qquad (9)$$

In eqn. 9, TZ is the determined value for a particular homologous pair average $\overline{CH}$ [*e.g.*, $(C_{12} + C_{13})/2 = C_{12.5}$]. Eqn. 9 was shown to be valid for a homologous series of straight-chain alkanes, carboxylic acids, methyl esters and alcohols with correlation coefficients of >0.95 [15]. A point of concurrence of these equations for each compound class was obtained at a TZ value of *ca.* -1. Eqns. 5 and 6 predict that when the retention times of a and b are equal ($t_r^b = t_r^a$), then $\alpha = 1$, no separation occurs and TZ would equal -1. It was found that the largest TZ values and absolute slopes were obtained with low TPRs and initial flow-rates of *ca.* 0.85 ml/min for a 12 m $\times$ 0.25 mm I.D. fused silica SP-2100-coated column.

A subsequent TPR study of the effect on the TZ values of six homologous *n*-alkanes (C_{12}–C_{17}) at starting temperatures of 40, 50 and 60°C under constant head pressure (isobaric flow) or constant flow-rate (maintained by pressure programming) [16] showed that (1) the slope values of eqn. 9 were more negative for isobaric flow than they were for constant flow; (2) CH_C values for isobaric flow were unique to the starting temperature/starting flow-rate/TPR, increasing with increasing flow-rate and starting temperature; (3) under constant flow conditions only one CH_C per starting temperature was observed for all flow-rates/TPRs; and (4) TZ values were optimized at a starting temperature of 40°C and a TPR of 1°C/min with flow-rates of 0.95 ml/min for isobaric flow and 0.89 ml/min for constant flow.

In 1962, Purnell [17] stated that flow programming could lead to chromatographic separations comparable to those obtained by TPGC. Zlatkis *et al.* [18], using a combination of temperature programming and flow programming (*i.e.*, double programming), reduced the time of a capillary column separation of an alkylbenzene mixture to 26 min from the 45 min required when using TPGC alone. Nygren [19] investigated the efficacy of double programming and stated that "flow and temperature programming can be used together in order to maximize the separating power of a capillary column". Ettre *et al.* [20] noted that as the temperature increases from temperature programming, k' will decrease for the same solute resulting in a larger μ_{opt} at higher temperatures. (This temperature dependence of μ_{opt} was observed in our recent study of h and TZ values at 40, 60 and 80°C [14].) Then, for double programming, chromatographic conditions would be conceivably less removed from the optimum than if pressure programming were performed isothermally. These statements, in conjunction with our previous work [14–16] suggested that a study of the changes in TZ as a function of several different pressure programming rates (PPR) superimposed on selected temperature programming rates (TPR) with low starting temperatures might provide further insight into the utility of TZ in capillary column optimization.

The previous approach of relating the initial flow to the TZ of each $\overline{CH}$ [15,16] was deemed inappropriate because, with double programming, the flow-rate was changing with a concomitant change in

temperature. Under TPGC and isobaric or constant flow conditions, each solute elutes at a particular temperature which can be determined by multiplying the *TPR* by the t_r of that solute and adding the result to the starting temperature. Perry [21] defined this temperature as the retention temperature. A similar approach was proposed by Ettre *et al.* [20] in defining elution flow. In isothermal linear carrier gas flow programming, the flow existing at the time the solute elutes (the elution flow-rate, F_e) is defined as being equal to the sum of the initial flow-rate, F_i, plus the product of the solute's t_r and the flow programming rate, r, in ml/min:

$$F_e = F_i + t_r(r) \quad (10)$$

As pressure can be related to flow, an analogous equation for determining the existing head pressure at the time the solute elutes (P_e) can be calculated from the sum of the initial pressure (P_i) and the *PPR* (t_r) product and the pressure related to flow:

$$P_e = P_i + t_r(PPR) \quad (11)$$

As shown previously, the optimum flow for TZ_{max} is determined by the average of the optimum flow of the two homologues [14], and therefore by similar averaging of F_e for these homologues, the calculated F_e for *TZ* and $\overline{CH}$ can be determined.

This paper reports that the *TZ* value for each $\overline{CH}$ can be related to its F_e in a Van Deemter-type equation similar to that derived previously [14]. From this relationship, the optimum starting flow-rate and the optimum *PPR* for the selected starting temperature of 40°C and selected *TPR* can be determined.

EXPERIMENTAL

A Hewlett-Packard Model 5880A gas chromatograph equipped with a Model 7671 autosampler, a flame ionization detector, an electronic flow control, a split splitless injector set for a splitting ratio of 1:200 and a Level IV microprocessor with an alphanumeric keyboard was used. Helium was utilized as the carrier gas. The "report annotation" mode presented electronically measured values of retention times (±0.10 min) and peak widths at half-height ($w_{0.5}$) repeatable to ±1% [15]. Through "run time" commands at 5-min intervals, a print-out on the chromatogram of the actual column head pressure and its set-point, followed by the actual column/oven temperature and its set-point, provided a constant indication of the linearity of the temperature and pressure programming. On completion of the run, a specifically designed BASIC program listed the GC parameter settings for the particular run (*i.e.*, for oven temperature, initial value, 1-min hold, temperature programming rate, final oven temperature; for column head pressure, initial value, 1-min hold, pressure programming rate, final value; split flow value) and the calculated *TZ* values between the C_{12}–C_{17} *n*-alkane homologues (peaks 1 and 2; 2 and 3; 3 and 4; 4 and 5; 5 and 6).

The six *n*-alkanes used were 99+% pure *n*-dodecane, *n*-tridecane, *n*-tetradecane, *n*-pentadecane, *n*-hexadecane and *n*-heptadecane from Alltech (Applied Science Labs., Deerfield, IL, USA). Approximately 0.3 g of each alkane was weighed and the combined weights made up to 10 ml with high-performance liquid chromatographic grade chloroform. A 1-ml aliquot diluted to 50 ml produced a concentration which resulted in on-scale peaks at an attenuation of 0 for 5-μl injections at the splitting ratio of 1:200.

A cross-linked DB-5 fused-silica capillary column of film thickness 0.25 μm (15 m × 0.248 mm I.D.) (J&W Scientific, Rancho Cordova, CA, USA) was used and was conditioned by microprocessor-controlled repeated TPGC runs from 100 to 200°C at 10°C/min with a helium head pressure of 75 kPa for 2 days. When not in operation, the column was continuously purged at 250°C with helium at *ca.* 0.5 ml/min. The maximum temperature was never allowed ot exceed 250°C, although the manufacturer's recommended maximum temperature was 325°C for isothermal operation. All runs were performed with injection port and detector temperatures set at 275°C with the starting temperature for all runs set at 40°C. Head pressures of 50, 75, 100 and 125 kPa provided initial helium flow-rates (F_i) of 0.677, 1.10, 1.49 and 1.88 ml/min. These, and all other helium flow-rates required for this study, were determined by substituting the t_r of injected butane and into the equation $F = \pi r^2 L/t_r$, where r (cm) is the radius of a column of length L (cm). The *PPR* required to maintain a constant flow-rate during a particular *TPR* was experimentally determined. All other *PPR*s used with an individual *TPR* were chosen to be geometric multiples of the *PPR* re-

quired to maintain a constant flow-rate. In no instance did the pressure required within the run time exceed the previously determined limits of the flow control unit.

Flow-rates for each *PPR* applied to a specific *TPR* were determined by a linear regression of temperature *versus* flow-rate, as described below. The flow-rate was experimentally determined at four temperature points for each *PPR*; the initial conditions of temperature and pressure, two points representing one third and two thirds of the temperature increase of the run time and a final point at a temperature and pressure beyond those required to elute the final alkane, thus ensuring a known range of flow-rates greater than those achieved during the run. At each of these four points, duplicate butane injections were made, flow-rates were calculated as described above and substituted into the equation $F = a(T - 40) + F_i$, where F is the calculated flow-rate, T is the set column temperature and F_i is the measured flow-rate at 40°C and the initial head pressure. Fig. 1 shows the linear regressions of the

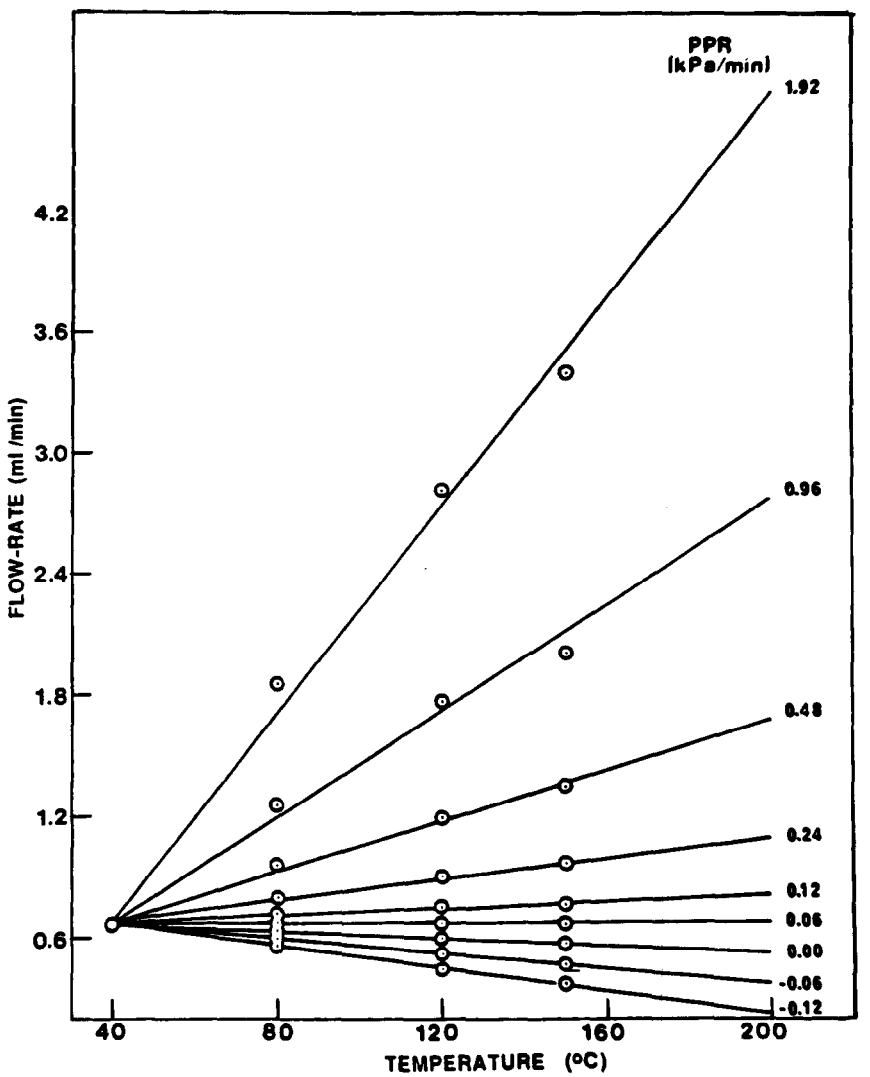

Fig. 1. Flow-rates generated by the indicated *PPR*s imposed on a *TPR* of 0.90°C/min, starting temperature 40°C and starting flow-rate 0.677 ml/min. Equations given in Table I.

TABLE I

COEFFICIENTS FOR THE EQUATION F = SLOPE (T-40) + F_i FOR STARTING TEMPERATURE = 40°C, *TPR* = 0.90°C/min, INITIAL PRESSURE, 50 kPa (0.677 ml/min) FOR VARIOUS *PPR*s[a]

TPR (°C/min)	*PPR* (kPa/min)	Initial flow-rate (ml/min)	Concurrent regression slope (S.D.)	Point of concurrence *y*-intercept point T	Flow-rate at 225°C (ml/min)[b]
0.90	1.92	0.677	$2.57 \cdot 10^{-2}$ ($7.91 \cdot 10^{-4}$)	40.0	5.43
	0.96		$1.31 \cdot 10^{-2}$ ($3.41 \cdot 10^{-4}$)	40.0	3.10
	0.48		$6.28 \cdot 10^{-3}$ ($1.45 \cdot 10^{-4}$)	40.0	1.84
	0.24		$2.74 \cdot 10^{-3}$ ($7.07 \cdot 10^{-5}$)	40.0	1.18
	0.12		$9.35 \cdot 10^{-4}$ ($4.26 \cdot 10^{-5}$)	40.0	0.846
	C.F.[c] 0.06		$-2.99 \cdot 10^{-5}$ ($2.80 \cdot 10^{-6}$)	40.0	0.679
	0.00		$-8.99 \cdot 10^{-4}$ ($5.69 \cdot 10^{-6}$)	40.0	0.507
	−0.06		$-1.85 \cdot 10^{-3}$ ($1.35 \cdot 10^{-5}$)	40.0	0.331
	−0.12		$-2.76 \cdot 10^{-3}$ ($2.70 \cdot 10^{-5}$)	40.0	0.162

[a] T = Selected column temperature; F_i = initial flow-rate. All $R^2 \geqslant 0.992$.
[b] Flow-rate predicted at 225°C from regression equation.
[c] C.F., *PPR* required for constant flow-rate.

relationship between flow-rate and temperature at the indicated *PPR*s for a starting pressure of 50 kPa (0.677 ml/min) and a starting temperature of 40°C at a *TPR* of 0.90°C/min, selected for discussion here. Deviations from linearity became apparent at the higher *PPR*s of 0.96 and 1.92. Table I lists the regression coefficients obtained for these data. The experimentally determined flow-rates for 225°C are included to insure the linearity of the relationship. All R^2 values were at least 0.992. Similar equations were generated for all starting flows and all *TPR*–*PPR* combinations used.

In order to develop the Van Deemter-type relationship, it was necessary to calculate the elution flow-rate, F_e, or the flow-rate existing at the time of elution of $\overline{CH}$ for which *TZ* was calculated. As each hydrocarbon eluted at a characteristic retention time and elution temperature, T_e, dependent on the *TPR*–*PPR* combination used, the determination of T_e for each *TZ* required the averaging of the t_rs of the homologous pair used in calculating the *TZ* value (eqn. 5). As an example, averaging of the t_rs for C_{12} and C_{13} provides the "retention time" for $\overline{CH}$, the average hydrocarbon $C_{12.5}$. Thus, knowing the *TPR* (in this instance 0.90°C/min) and the initial column temperature, one need only know the superimposed *PPR* and, from the appropriate *PPR* line in Fig. 1 or the corresponding equation in Table I, one can calculate the elution flow-rate, F_e, the column flow-rate at the t_r for $\overline{CH}$.

RESULTS AND DISCUSSION

In the previous work relating h and *TZ* [14], a range of constant flow-rates were utilized at isothermal temperatures of 40, 60 and 80°C, the appropriate Van Deemter-type equations were determined and from these equations the optimum flow-rates required to produce minimum h or maximum *TZ* values were calculated. In this work, the objective was to determine not only the *PPR* necessary to provide the maximum *TZ* values for each $\overline{CH}$, but also the optimum starting flow-rates at selected *TPR*s. Hence the starting flow-rates were set by initial head pressures of 50, 75, 100 and 125 kPa, the same as used previously [16], and also the same *TPR*s except that, for the 50-kPa study, two additional rates of 0.90 and 1.80°C/min were added. The starting temperature of 40°C was employed as maximum *TZ* values were obtained with low *TRP*s and starting flow-rates of *ca.* 0.80 ml/min [16].

After concluding this study utilizing all the *TPR*s at the different head pressures (five *TPR*s for 50 kPa and four *TPR*s for 75, 100 and 125 kPa), it was

determined that within each head pressure or flow set, the lowest *TPR* provided the largest *TZ* values using all the superimposed *PPR*s and only these results are shown here. Table II summarizes the *TZ* values and the elution flow-rates, F_e, calculated for each $\overline{CH}$ determined for all *PPR*s superimposed on the lowest *TPR* for each starting head pressure/flow-rate.

Relationship between TZ and PPR

Initially, the *TZ* values for each $\overline{CH}$ obtained were plotted *versus* those *PPR*s used with a starting flow-rate of 50 kPa, 0.677 ml/min, at a *TPR* of 0.90°C/min (as shown in Table II). The plots thus obtained were parabolic curves which fit the model $TZ = a(PPR)^2 + b(PPR) + c$. The coefficients were determined for each $\overline{CH}$, the equations differ-

TABLE II

TZ VALUES AND ELUTION FLOW-RATES, F_e, FOR ALL $\overline{CH}$s AS A FUNCTION OF THE *PPR*s IMPOSED ON THE LOWEST *TPR*s OF INDICATED STARTING PRESSURES AND FLOW-RATES

PPR	Conditions[a]	$\overline{CH}$									
		12.5		13.5		14.5		15.5		16.5	
		TZ	F_e	*TZ*	F_e	*TZ*	F_e	*TZ*	F_e	*TZ*	F_e
1.92	A	34.47	1.487	30.00	1.725	26.07	1.965	22.63	2.202	19.73	2.434
0.96		37.83	1.138	34.25	1.271	30.89	1.403	27.74	1.532	25.04	1.657
0.48		38.82	0.917	35.93	0.986	33.10	1.053	30.50	1.119	28.21	1.182
0.24		38.66	0.787	36.07	0.819	33.49	0.850	31.18	0.880	29.10	0.909
0.12		38.31	0.716	35.72	0.727	33.21	0.738	30.87	0.749	28.85	0.759
0.06	C.F.[b]	37.84	0.678	35.16	0.679	32.56	0.679	31.39	0.679	28.30	0.680
0.00		37.76	0.638	35.31	0.627	32.67	0.616	30.28	0.605	28.10	0.595
−0.06		37.52	0.596	34.83	0.572	32.39	0.548	29.85	0.525	27.48	0.503
−0.12		37.18	0.554	33.95	0.516	31.06	0.479	28.34	0.443	25.67	0.409
2.79	B	30.05	1.898	26.00	2.135	22.61	2.370	19.66	2.601	17.27	2.825
1.40		33.09	1.527	29.65	1.635	26.60	1.777	23.87	1.898	21.61	2.014
0.70		34.95	1.304	31.95	1.364	29.35	1.423	26.85	1.480	24.64	1.535
0.35		35.85	1.180	33.22	1.203	30.67	1.227	28.43	1.249	26.50	1.271
0.17	C.F.[b]	36.37	1.142	33.79	1.154	31.50	1.167	29.30	1.178	27.34	1.190
0.00		36.49	1.038	34.11	1.020	31.81	1.001	29.68	0.983	27.77	0.967
−0.17		36.70	0.966	34.31	0.925	32.04	0.884	29.88	0.845	27.93	0.808
−0.35		37.10	0.833	34.38	0.814	32.03	0.747	29.64	0.681	27.36	0.617
2.24	C	27.72	2.280	23.81	2.576	20.47	2.880	17.79	3.180	15.59	3.473
1.12		30.13	1.973	27.11	2.157	24.28	2.342	21.64	2.523	19.33	2.699
0.56		32.09	1.715	29.33	1.801	26.84	1.889	24.53	1.974	22.47	2.055
0.28		32.87	1.573	30.40	1.605	28.12	1.638	26.60	1.670	24.13	1.700
0.14	C.F.[b]	33.21	1.499	30.86	1.503	28.81	1.507	26.87	1.510	25.06	1.514
0.00		33.71	1.420	31.61	1.392	29.67	1.364	27.75	1.336	26.14	1.310
−0.14		34.01	1.337	32.19	1.276	30.43	1.214	28.77	1.154	27.30	1.095
−0.28		34.89	1.250	32.85	1.153	31.27	1.054	29.16	0.956	28.13	0.862
1.02	D	27.59	2.253	24.68	2.427	22.02	2.610	19.62	2.792	17.40	2.970
0.51		29.12	2.054	26.67	2.137	24.40	2.224	22.48	2.311	20.54	2.394
0.26		29.80	1.944	27.74	1.975	25.69	2.008	23.77	2.040	22.08	2.072
0.13	C.F.[b]	29.90	1.887	28.05	1.891	26.20	1.894	24.39	1.898	22.78	1.902
0.00		30.36	1.825	28.55	1.798	26.91	1.769	25.20	1.741	23.83	1.714
−0.13		30.45	1.762	28.94	1.703	27.52	1.641	26.04	1.579	24.80	1.519
−0.26		30.88	1.692	29.54	1.598	28.30	1.498	27.24	1.398	26.22	1.300

[a] (A) 50 kPa, F_i = 0.677 ml/min, *TPR* 0.90°C/min; (B) 75 kPa, F_i = 1.10 ml/min, *TPR* 1.35°C/min; (C) 100 kPa, F_i = 1.49 ml/min, *TPR* 0.86°C/min; (D) 125 kPa, F_i = 1.88 ml/min, *TPR* 0.60°C/min.

[b] C.F. = The *PPR* required for constant flow-rate.

entiated as described previously [14], and optimum *PPR*s were determined. From these optimum *PPR*s, the maximum *TZ* values were calculated by substitution in the appropriate original equation. The coefficients obtained for each $\overline{CH}$, the PPR_{opt} and TZ_{max} and correlation coefficients are summarized in Table III.

As shown in Table III, TZ_{max} values decrease and PPR_{opt} become smaller as $\overline{CH}$ increases. However, it is apparent that no single *PPR* would provide TZ_{max} for all the $\overline{CH}$s used in this study and no information was available to calculate an optimum starting flow-rate. As a consequence, this approach was abandoned.

Relationship between TZ and F_e

The relationship between *TZ* and F_e was investigated next. When *TZ* was plotted *vs.* the elution flow-rate (F_e) at a particular *TPR* for each $\overline{CH}$, a parabolic curve resulted when the initial flow-rate and *TPR* were low. As the initial flow-rates increased, the parabolicity diminished and increasingly straight lines with negative slopes were observed. Using the data from Table II, the relationship between *TZ* and F_e for all *PPR*s at the lowest *TPR* for each of the following initial pressure/starting flows are shown: Fig. 2 for 50 kPa, 0.677 ml/min, *TPR* 0.90°C/min; Fig. 3 for 75 kPa, 1.10 ml/min, 1.35°C/min; Fig. 4 for 100 kPa, 1.49 ml/min, 0.86°C/min; and Fig. 5 for 125 kPa, 1.88 ml/min, 0.60°C/min. In these plots, the *TZ* values for each $\overline{CH}$ obtained at a particular *PPR* are connected by straight lines, giving rise to the "fan-like" appearance.

Low initial flow-rates, *i.e.*, 0.677 ml/min (50 kPa, Fig. 2) and 1.10 ml/min (75 kPa, Fig. 3), resulted in a parabolic relationship between *TZ* and F_e for each $\overline{CH}$ (similar to the *TZ vs.* flow-rate plot obtained in the isothermal study of the effect of flow-rate on *h* and *TZ* [14]). It is apparent that an optimum flow-rate produces maximum *TZ* values. Above the optimum flow-rate, the *TZ* values decrease owing to band broadening resulting from increased resistance to mass transfer. At flow-rates less tham the optimum, the *TZ* values decrease owing to longitudinal diffusion band broadening. For *TPR*s using the higher initial flow-rates of 1.49 ml/min (100 kPa, Fig. 4) and 1.88 ml/min (125 kPa, Fig. 5), the parabolic curvature flattens. A negative *PPR* producing decreasing flow-rates from high starting flow-rates improved the *TZ* values, although they were still significantly lower than those obtained at starting flow-rates of 0.677 ml/min (Fig. 2) or

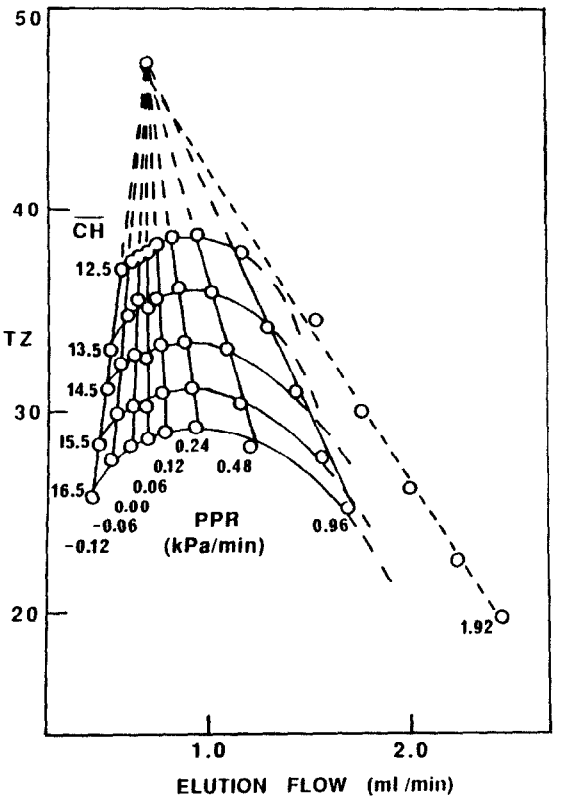

Fig. 2. Elution flow-rate for the *TZ* value of each $\overline{CH}$ for the homologous series C_{12}–C_{17} under the conditions of starting flow-rate 0.677 ml/min (50 kPa), *TPR* of 0.90°C/min and *PPR*s as indicated. Data from Table II.

TABLE III

COEFFICIENTS FOR THE EQUATION $TZ = a(PPR)^2 + b(PPR) + c$ USING THE DATA FROM TABLE II FOR 50 kPa, F_i = 0.677 ml/min, *TPR* 0.90°C/min

$\overline{CH}$	a	b	c	R^2	PPR_{opt}	TZ_{max}
12.5	−2.38	2.79	37.79	0.962	0.586	40.03
13.5	−2.76	2.58	35.05	0.932	0.467	36.86
14.5	−2.89	2.12	32.45	0.929	0.367	33.50
15.5	−3.00	1.78	30.02	0.910	0.297	30.72
16.5	−3.22	1.29	27.76	0.884	0.283	28.45

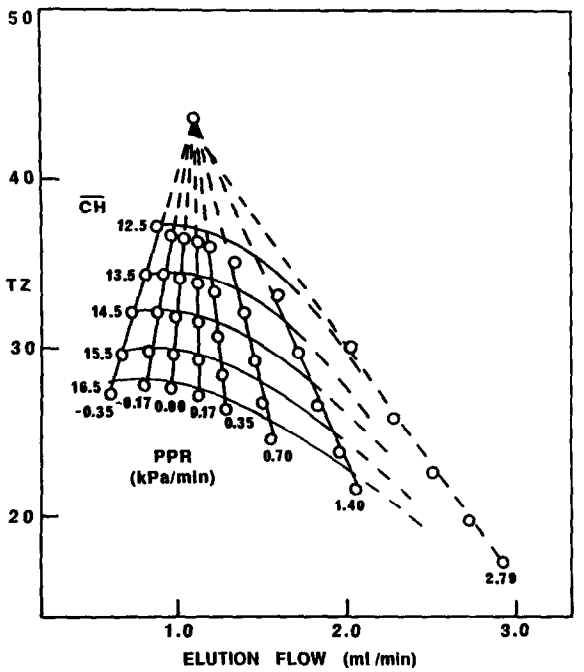

Fig. 3. Elution flow-rate for the *TZ* value of each $\overline{CH}$ for the homologous series C_{12}–C_{17} under the conditions of starting flow-rate 1.10 ml/min (75 kPa), *TPR* of 1.35°C/min and *PPR*s as indicated. Data from Table II.

1.10 ml/min (Fig. 3). As only resistance to mass transfer was operating at these high initial flow-rates, an increasing flow-rate produced larger $w_{0.5}$ values and decreasing *TZ* values, resulting in a negative slope for each $\overline{CH}$'s relationship between *TZ* and F_e. A model which adequately describes both the parabolic relationship at low initial flow-rates and the linear relationship at high initial flow-rates is the quadratic equation

$$TZ = x(F_e)^2 + y(F_e) + z \quad (12)$$

Table IV lists the coefficients, their standard deviations for each $\overline{CH}$ for all the *TPR*–*PPR* combinations studied in the 50- and the 125-kPa groups. The 75- and 100-kPa data have been omitted from Table IV as it is clear from Figs. 4 and 5 that higher flow-rates result in the parabolic curve being flattened with the result that the squared term, F_e^2, becomes insignificantly different from zero [as indicated by the large standard deviation for the coefficient x for the 125-kPa data (Table IV)].

Laminar and turbulent flow and their effects on TZ

The flow profile in a column can be either laminar or turbulent [22,23]. Most chromatographic separa-

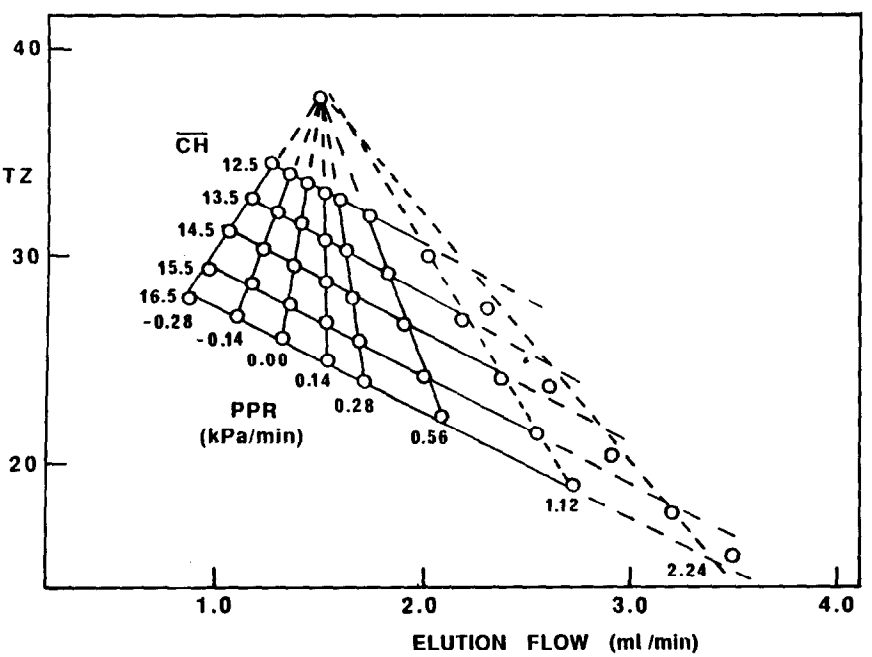

Fig. 4. Elution flow-rate for the *TZ* value of each $\overline{CH}$ for the homologous series C_{12}–C_{17} under the conditions of starting flow-rate 1.49 ml/min (100 kPa), *TPR* of 0.86°C/min and *PPR*s as indicated. Data from Table II.

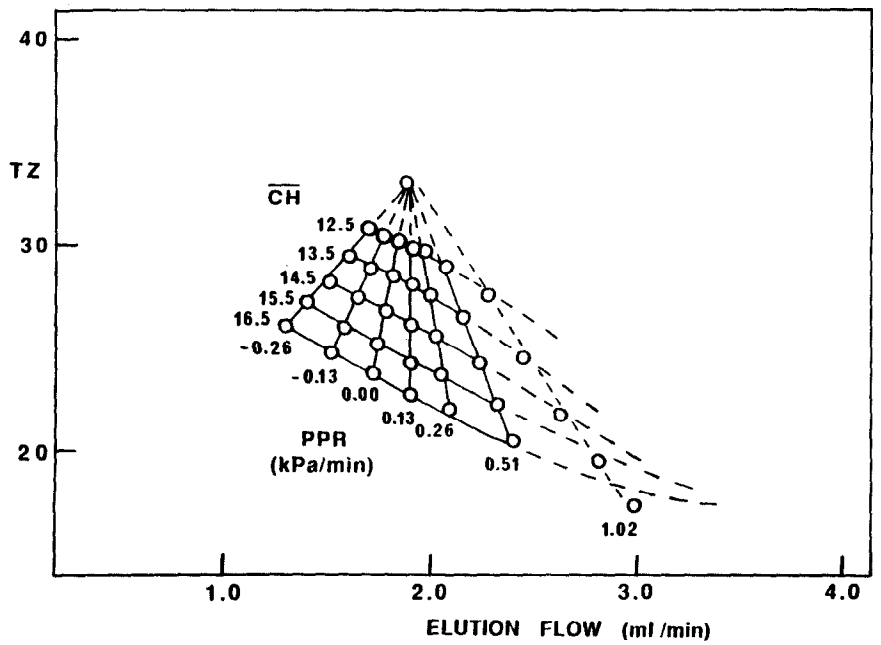

Fig. 5. Elution flow-rate for the *TZ* value of each $\overline{CH}$ for the homologous series C_{12}–C_{17} under the conditions of starting flow-rate 1.88 ml/min (125 kPa), *TPR* of 0.60°C/min and *PPR*s as indicated. Data from Table II.

tions are performed using low flow-rates, which provide a laminar flow profile characterized by a parabolic or "bullet-shaped" flow front. Minimum radial mixing occurs with a laminar flow profile and a solute molecule will, ideally, not deviate from the straight-line path it follows throughout the column. Carrier gas velocity varies with radial position, that is, the velocity at the center of the tube (μ_c) which is slightly faster than the velocity at the tube's inner wall (μ_w). For a straight cylindrical column, the velocity $\mu(r)$ varies with the distance from the center of the column as

$$\mu(r) = 2\mu[1 - (r/R)^2] \tag{13}$$

where r is the radial coordinate (distance from the center of the column), R is the column radius and μ is the mean velocity. The different velocities of each flow path result in peak broadening as the sample molecules at various distances from the column's center reach the detector over a period of time. As flow-rates increase, the onset of turbulent flow occurs when radial mixing flattens the leading edge of the profile and breaks down the parabolic shape [22]. The change in a flow profile from purely laminar to purely turbulent flow is not well defined. The Reynolds number (*Re*) reflects the onset of turbulence. When $Re \lesssim 2100$, flow is purely laminar, and when $Re \gtrsim 4000$, flow is purely turbulent [23]. The Reynolds number is defined by

$$Re = \frac{2\rho\mu R}{n} \tag{14}$$

where ρ (g/cm^3) is the density of the fluid (*i.e.*, the carrier gas), μ (cm/s) is the carrier gas linear velocity, n (μP) is the viscosity of the fluid and R (cm) is the column radius. The continuous radial mixing of the solute molecules associated with turbulent flow has an adverse effect on the ability of the solute to partition between the mobile and stationary phases and results in an increasing deviation in the relationship between *TZ* and F_c as a function of *PPR*.

The high flow-rates that arise from fast positive *PPR*s, especially those resulting in a non-laminar flow profile, result in decreased k' values, larger peak widths and decreased *TZ* values. Martin and Guiochon [24] noted in their study of band broadening in

TABLE IV

COEFFICIENTS AND STANDARD DEVIATIONS FOR THE QUADRATIC REGRESSIONS FOR *TZ VS.* ELUTION FLOW-RATE, F_e, FOR EACH *TPR* OF EACH $\overline{CH}$ FOR THE EQUATION $TZ = x(F_e)^2 + y(F_e) + z$

P_i (kPa)[a]	F_i (ml/min)[b]	*TPR* (°C/min)	$\overline{CH}$	Coefficient			R^2
				x (S.D.)	*y* (S.D.)	*z* (S.D.)	
50	0.677	0.90	12.5	−14.5 (1.48)	25.8 (2.51)	27.2 (1.01)	0.961
			13.5	−13.4 (1.33)	24.2 (2.39)	25.2 (0.995)	0.954
			14.5	−10.9 (1.31)	20.0 (2.49)	24.3 (1.07)	0.935
			15.5	−9.77 (1.00)	18.3 (2.01)	22.6 (0.882)	0.954
			16.5	−8.93 (1.01)	17.4 (2.12)	20.6 (0.952)	0.945
50	0.677	1.80	12.5	−20.5 (1.31)	37.3 (2.31)	19.7 (0.954)	0.982
			13.5	−17.5 (2.08)	32.8 (3.90)	18.9 (1.65)	0.934
			14.5	−14.6 (1.91)	28.7 (3.77)	18.1 (1.64)	0.922
			15.5	−11.7 (1.42)	23.9 (1.31)	17.5 (2.94)	0.932
			16.5	−10.1 (1.35)	21.0 (2.94)	16.6 (1.34)	0.918
50	0.677	3.60	12.5	−16.7 (1.11)	34.0 (2.07)	16.2 (0.864)	0.980
			13.5	−14.3 (1.35)	30.3 (1.13)	15.2 (2.65)	0.960
			14.5	−12.7 (1.21)	27.8 (2.49)	14.0 (1.09)	0.950
			15.5	−11.1 (1.03)	25.0 (2.22)	13.1 (0.989)	0.949
			16.5	−9.75 (1.12)	22.8 (2.51)	12.2 (1.13)	0.922
50	0.677	7.20	12.5	−15.1 (1.19)	33.8 (2.35)	11.3 (1.02)	0.977
			13.5	−13.6 (1.02)	31.3 (2.12)	10.1 (0.943)	0.972
			14.5	−11.4 (1.05)	27.2 (2.30)	9.97 (1.04)	0.953
			15.5	−9.76 (1.06)	13.9 (2.42)	9.73 (1.12)	0.929
			16.5	−8.66 (0.912)	21.9 (2.18)	9.09 (1.02)	0.928
50	0.677	14.40	12.5	−19.6 (1.04)	44.2 (1.73)	1.20 (0.672)	0.998
			13.5	−18.1 (0.829)	41.1 (1.42)	0.859 (0.556)	0.998
			14.5	−17.7 (0.861)	39.8 (1.51)	0.135 (0.594)	0.997
			15.5	−16.2 (0.538)	36.7 (0.962)	0.235 (0.382)	0.998
			16.5	−13.9 (0.337)	32.3 (0.615)	0.965 (0.245)	0.999
125	1.88	0.60	12.5	−1.99 (3.24)	2.76 (1.22)	31.9 (11.4)	0.981
			13.5	−1.48 (1.16)	3.62 (4.33)	32.7 (4.02)	0.996
			14.5	−0.511 (0.399)	−3.41 (1.49)	34.5 (1.37)	0.999
			15.5	0.618 (0.459)	−7.61 (1.71)	36.6 (1.53)	0.998
			16.5	0.899 (0.263)	−8.45 (0.975)	35.6 (0.878)	0.999
125	1.88	1.20	12.5	−2.19 (4.73)	1.30 (1.69)	34.0 (15.1)	0.972
			13.5	−0.212 (2.64)	−5.54 (9.25)	37.9 (8.08)	0.982
			14.5	−0.192 (1.64)	−5.44 (5.65)	35.9 (4.81)	0.988
			15.5	−1.17 (0.823)	−1.62 (2.78)	30.5 (2.31)	0.995
			16.5	−0.0931 (0.644)	−2.47 (2.13)	29.6 (1.73)	0.995
125	1.88	2.40	12.5	−2.71 (1.45)	4.44 (5.12)	29.0 (4.50)	0.988
			13.5	−2.34 (1.07)	2.96 (3.68)	28.5 (3.17)	0.989
			14.5	−1.46 (0.609)	0.0519 (2.06)	29.3 (1.73)	0.995
			15.5	−0.782 (0.308)	−2.56 (1.02)	29.8 (0.837)	0.998
			16.5	−0.664 (0.221)	−2.87 (0.717)	28.5 (0.575)	0.999
125	1.88	3.60	12.5	1.01 (1.54)	−9.68 (5.38)	41.1 (4.67)	0.987
			13.5	0.782 (1.15)	−8.63 (3.91)	37.9 (3.32)	0.988
			14.5	0.619 (0.578)	−7.68 (1.93)	35.0 (1.59)	0.977
			15.5	0.233 (0.417)	−5.21 (1.35)	30.8 (1.08)	0.995
			16.5	−0.595 (0.429)	−3.02 (1.37)	27.5 (1.08)	0.993

[a] Initial pressure.
[b] Initial flow-rate.

TABLE V

PEAK WIDTHS AT HALF-HEIGHT FOR C_{12} AND C_{17} AND REYNOLDS NUMBERS AT EACH *PPR* OF THE *TPR* 0.90°C/min INITIAL FLOW-RATE 0.677 ml/min

	PPR (kPa/min)	C_{12}		C_{17}	
		$w_{0.5}$	*Re*	$w_{0.5}$	*Re*
	1.92[a]	0.131	967	0.252	2236
	0.96	0.137	543	0.205	981
	0.48	0.147	347	0.189	489
	0.24	0.159	254	0.193	289
	0.12	0.168	210	0.200	202
C.F.[b]	0.06	0.173	189	0.208	163
	0.00	0.177	168	0.214	126
	−0.06	0.186	147	0.224	92
	−0.12	0.189	127	0.259	63

[a] Turbulent flow-rates for some CH values.
[b] *PPR* for constant flow-rate.

turbulent flow GC that the plate height increases with increasing gas velocity, indicating an increase in $w_{0.5}$ as shown in Table V. This effect was most evident for the high-molecular-weight solutes and Table V compares the peak widths at half-height of the C_{12} and C_{17} alkanes at all of the *PPR*s of the *TPR* 0.90°C/min, initial flow-rate 0.677 ml/min group. Also attributed to turbulent flow is the deviation from linearity in the relationship between flow-rate and temperature (Fig. 1) at fast *PPR*s when the onset of turbulent flow increases the resistance to flow. This is reflected by the increasing standard deviation in the slope (Table I) as the *PPR* was increased in all *TPR–PPR* combinations considered.

Relationship between TZ and F_e for each $\overline{CH}$ produced by a single PPR

As shown in Table II, the most negative *PPR*, −0.12 kPa/min, resulted in the lowest elution flow-rates for this *TPR* of 0.90°C/min, and produced the largest peak width for C_{17} ($w_{0.5}$ = 0.259), because of longitudinal diffusion (Table V). As the *PPR* was increased, the peak width values decreased (longitudinal diffusion minimized), and at the *PPR* of 0.48 kPa/min, a minimum value ($w_{0.5}$ = 0.189) was attained for C_{17}. On doubling the *PPR* to 0.96 kPa/min, the resistance to mass transfer increased and the peak width increased by 8.5% to 0.205. When the *PPR* was doubled again, however, to 1.92 kPa/min, non-laminar or turbulent flow-rates were produced (*Re* = 2236) and the peak width increased by 23% to value of 0.252, approximating that of the *PPR* −0.12 kPa/min. Conversely, as the effects of flow-rate changes are most evident for high-molecular-weight solutes, the peak widths for C_{12} did not exhibit the same pattern as those for C_{17}. At the *PPR* of −0.12 kPa/min, the $w_{0.5}$ value for C_{12} was 0.189, which decreased as the *PPR* increased to its maximum of 1.92 kPa/min.

In the Figs. 2–5, each point representing a *TZ* value and its associated F_e is connected horizontally to produce the parabolic curves shown and described by eqn. 12. The standard deviations of the coefficients of the quadratic regressions increased when *PPR*s producing turbulent or near-turbulent flows were included in these calculations. Therefore, values of the coefficients for the quadratic regressions for each $\overline{CH}$ were determined for all *TPR*s omitting those *PPR*s which produce non-laminar flow-rates.

To determine the *TZ* and flow-rate values at the convergence of the vertical line in Figs. 2–5, it was necessary to determine the slopes of each *PPR* line.

As previously mentioned, only two initial flow-rates produced parabolic plots of the *TZ versus* F_e relationship for each $\overline{CH}$ (Fig. 2, F_i = 0.677 ml/min, and Fig. 3, F_i = 1.10 ml/min). Connecting the *TZ* values obtained for each $\overline{CH}$ of a selected single *PPR* resulted in a straight, near-vertical line or "rib". The lines thus obtained converge at a common *TZ* value which is a function of the original starting flow-rate and all such lines could be described by the equation

$$TZ = a(F_e) + b \qquad (15)$$

Considering only the data in Table II for the F_i of 0.677 ml/min with a *TPR* of 0.90°C/min and excluding the *PPR*s that gave rise to the non-laminar flow and that for constant flow (as under constant flow conditions *TZ* is not a function of flow), the remaining eight *PPR*s gave eight regression lines. The coefficients for eqn. 15 determined for the different starting flow-rates studied are summarized in Table VI.

Recognizing that these lines have a common *TZ* value at the point of concurrence, simultaneous solution of any pair of *PPR* lines for a selected *TPR*

TABLE VI

RELATIONSHIP $TZ = a(F_e) + b$ BETWEEN TZ AND LAMINAR ELUTION FLOW-RATES, F_e, FOR ALL $\overline{CH}$s IN THE VERTICAL LINES OF FIGS. 2–5 AS A FUNCTION OF ALL *PPR*s AT INITIAL FLOW-RATES AND *TPR*s

Conditions[a]	*PPR*	*a*	*b*	R^2
A	0.96	−24.72	65.76	0.998
	0.48	−40.22	75.59	0.999
	0.24	−78.76	100.57	0.999
	0.12	−220.20	195.80	0.999
C.F.[b]	0.06	−4770.00	3271.88	0.959
	0.00	225.51	−106.14	0.999
	−0.06	107.55	−26.61	0.999
	−0.12	78.90	−6.65	0.999
B	2.79	−13.76	55.68	0.992
	1.40	−23.31	68.04	0.993
	0.70	−44.53	92.83	0.998
	0.35	−103.10	157.83	0.998
C.F.[b]	0.17	−187.92	250.82	0.998
	0.00	122.21	−90.46	0.999
	−0.17	55.50	−16.98	0.999
	−0.35	41.54	1.43	0.963
C	1.12	−14.90	59.34	0.998
	0.56	−28.20	80.25	0.998
	0.28	−66.69	137.60	0.994
C.F.[b]	0.14	−547.86	854.36	0.998
	0.00	68.87	−64.19	0.999
	−0.14	27.80	−3.24	0.999
	−0.28	17.70	12.59	0.991
D	1.02	−14.14	59.17	0.997
	0.51	−25.00	80.23	0.997
	0.26	−60.46	147.21	0.998
C.F.[b]	0.13	−482.35	940.02	0.996
	0.00	58.82	−77.10	0.998
	−0.13	23.28	−10.64	0.999
	−0.26	11.80	10.77	0.995

[a] (A) 50 kPa, F_i = 0.677 ml/min, *TPR* 0.90°C/min; (B) 75 kPa, F_i = 1.10 ml/min, *TPR* 1.35°C/min; (C) 100 kPa, F_i = 1.49 ml/min, *TPR* 0.86°C/min; (D) 125 kPa, F_i = 1.88 ml/min, *TPR* 0.60°C/min.

[b] *PPR* required for constant flow-rate.

will yield the initial flow-rate which, when used in the original equation, will give the concurrent TZ value, TZ_c (method A). Alternatively, use of the known initial flow-rate will permit the calculation of TZ_c (method B). Thus, calculation by method A gives an average F_i of 0.669 ml/min (S.D. = 0.021) and using this F_i in the original equations gave a TZ_c value of 47.22 (S.D. = 1.84). Using method B with a constant flow-rate of 0.677 ml/min gives an average TZ of 47.27 (S.D. = 1.04). The values of F_i and TZ_c thus calculated for all *TPR–PPR* combinations reported here are given in Table VII. The agreement of the TZ_c values determined by both methods is acceptable, as is the agreement between the calculated F_i and that set experimentally.

Determination of TZ_{max}, $F_{e(opt)}$, new F_i and PPR

Previous studies [14,15] have shown that a quadratic relationship such as eqn. 12 can be differentiated to determine the maximum TZ and optimum flow-rate. For each $\overline{CH}$, a different quadratic model (excluding any *PPR*s resulting in non-laminar flow) was derived as shown in Table IV. Then, as described in the derivation of eqns. 3 and 4, differentiating eqn. 12 and setting the slope equal to zero gives

$$\frac{dTZ}{dF_e} = 2x\,(F_e) + y = 0 \qquad (16)$$

and the equation

$$F_{e(opt)} = -y/2x \qquad (17)$$

permits the calculation of the optimum F_e for that $\overline{CH}$. Substituting F_e into eqn. 12 and solving for TZ yields the TZ_{max} value for each $\overline{CH}$ [23]:

TABLE VII

COMPARISON OF TZ_c AND F_i CALCULATED BY METHODS A AND B

Conditions[a]		Method A		Method B
		F_i	TZ_c	TZ_c
A	Average[b]	0.668	47.22	47.27
	S.D.[c]	0.021	1.853	1.038
B	Average[b]	1.148	44.63	44.24
	S.D.[c]	0.087	4.511	1.526
C	Average[b]	1.515	38.26	38.20
	S.D.[c]	0.042	4.106	0.592
D	Average[b]	1.887	33.15	33.15
	S.D.[c]	0.027	0.456	0.353

[a] (A) 50 kPa, F_i = 0.677 ml/min, *TPR* 0.90°C/min; (B) 75 kPa, F_i = 1.10 ml/min, *TPR* 1.35°C/min; (C) 100 kPa, F_i = 1.49 ml/min, *TPR* 0.86°C/min; (D) 125 kPa, F_i = 1.88 ml/min, *TPR* 0.60°C/min.

[b] Average of eight determinations.

[c] Standard deviation of the averages.

TABLE VIII

THEORETICAL MAXIMUM *TZ* AND ITS ASSOCIATED $F_{e(opt)}$ UNDER THE CONDITIONS 50 kPa (F_i = 0.677 ml/min) AND A *TPR* OF 0.90°C/min, FROM THE DIFFERENTIATION OF $TZ = x(F_e)^2 + y(F_e) + z$ (EQN. 12)

$\overline{CH}$	TZ_{max}	$F_{e(opt)}$
12.5	38.68	0.892
13.5	36.13	0.899
14.5	33.47	0.914
15.5	31.17	0.935
16.5	29.09	0.973

$$TZ_{max} = (4xz - y^2)/4x \quad (18)$$

The resulting pairs of TZ_{max} and F_e values for the sample *TPR* 0.90°C/min, 50 kPa (F_i = 0.677 ml/min) are shown in Table VIII and are included in Fig. 6 as solid circles in an expanded plot of Fig. 2. Least-squares regression analysis [25] of the data in Table VIII gave the equation

$$TZ_{max} = -110.6\,(F_e) + 135.8 \quad (19)$$

with $R^2 \geqslant 0.900$.

Knowing that the TZ_C for a *TPR* of 0.90°C/min was 47.27 (Table VII), substitution of this value in eqn. 19 gave an F_i of 0.801 ml/min as the new initial flow-rate. This left only a comparison of the slope values of the regression equations describing the vertical lines or the "ribs" of the fans in Figs. 2 and 6 to determine the *PPR* necessary for the maximum *TZ* values for all the $\overline{CH}$s. The slope values *a* (eqn. 15) for *TZ* and F_e for all the *PPR* lines in Fig. 6 are shown in Table VI and, considering the extreme steepness of the slopes, the above value of −110.6 does not differ greatly from that of −220.4 obtained for the *PPR* of 0.12 kPa at 0.90°C/min (see below).

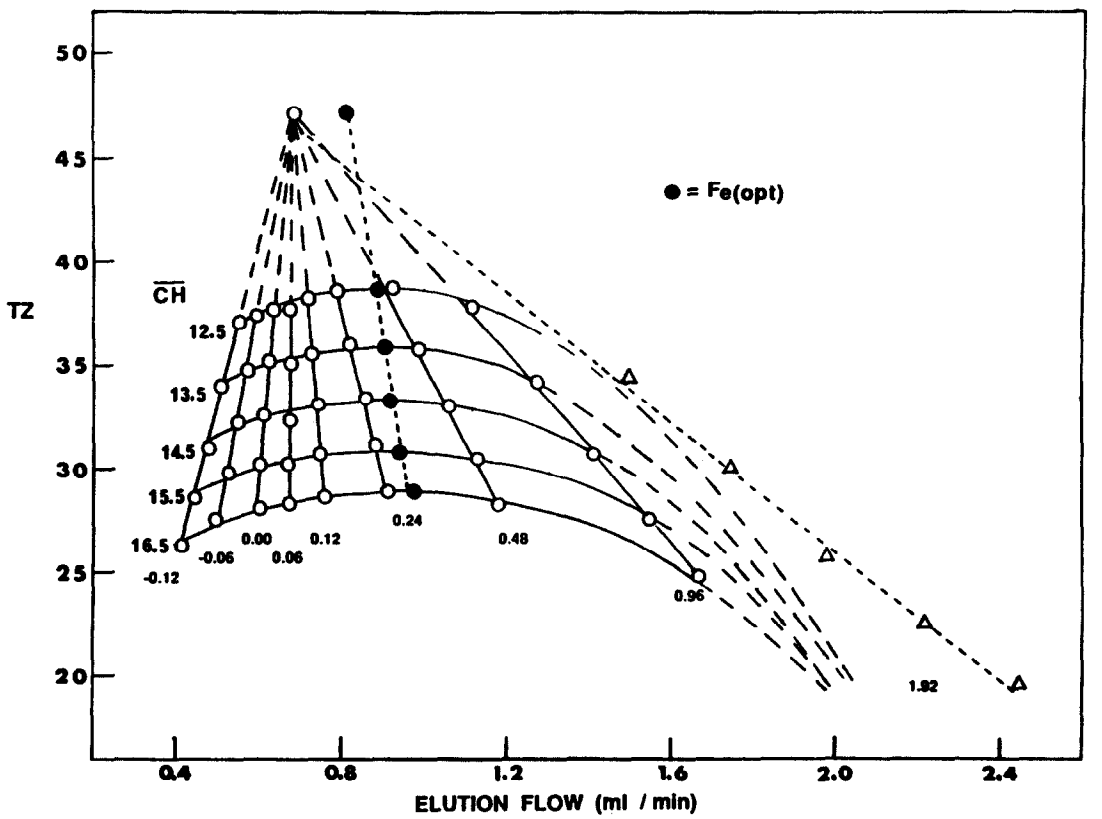

Fig. 6. Expanded version of Fig. 2. Solid circles connected by dashed line are *TZ* and F_e values calculated from eqns. 17 and 18 and are contained in Table VIII.

TABLE IX

COMPARISON OF PREDICTED *TZ* VALUES WITH THOSE EXPERIMENTALLY DETERMINED FOR STARTING FLOW-RATE OF 0.80 ml/min, *TPR* OF 0.90°C/min AND *PPR* OF 0.12 kPa/min

$\overline{CH}$	TZ_{max} (predicted)[a]	*TZ* (found)	$\frac{(TZ_{max} - TZ_{found})}{TZ_{max}} \cdot 100\,(\%)$
12.5	38.68	38.91	−0.595
13.5	36.13	36.35	−0.609
14.5	33.47	33.65	−0.538
15.5	31.17	31.27	−0.321
16.5	29.08	29.04	0.138

[a] See Table VIII.

Further, visual examination of Fig. 6 supports the conclusion that the slope of the new line parallels most closely that of the 0.12 kPa/min *PPR*.

To determine the efficacy and accuracy of the above determination, the C_{12}–C_{17} hydrocarbon mixture was again analyzed utilizing the new calculated starting flow-rate of 0.80 ml/min, a *TPR* of 0.90°C/min and a *PPR* of 0.12 kPa/min. Table IX compares the *TZ* values obtained with those predicted by the calculations as described above. The agreement between the predicted and experimentally determined *TZ* values is acceptable and appears to confirm the applicability of the approach.

The data shown in Table II which gave rise to the shallow parabolic curves (Fig. 6) illustrate that slight changes in the near-optimum *PPR*, as described above, produce small changes in the near-maximum *TZ*, as evidenced by the steep slopes shown in Table VI. To select the optimum velocity for the TPGC separation of a mixture of high- and low-molecular-weight solutes, Jennings [26] proposed a "velocity window" concept in which the optimum velocity is found to be intermediate to that required for the high partition ratio *k* solute (high *h*) and the low-*k* solute (low *h*). These values are proportional to low optimum velocity and high optimum velocity, respectively. The results shown here suggest that a similar "*PPR* window" exists for low *TPR*s and that for acceptable optimization, a *PPR* somewhere between isobaric flow (*PPR* = 0.0) and slightly positive *PPR* (+0.28 kPa/min) will provide a similar *TZ* maximization as shown in the above determination. The new calculated optimum starting flow-rate determined by using the *TPR–PPR* method described herein was *ca.* 0.80 ml/min, whereas by considering only [16] *TPR*, a starting constant flow-rate of 0.89 ml/min was previously calculated. Thus, for a 15 m × 0.25 mm I.D. column, a "*PPR* window" of 0–0.28 kPa/min with a starting flow-rate between 0.80 and 0.89 ml/min for either constant or isobaric flow will provide maximum or near-maximum *TZ* values for a *TPR* of 0.90°C/min.

ACKNOWLEDGEMENT

The authors are indebted to Mr. Terry Schmoeger of Hewlett-Packard for devising the software used to calculate *TZ* in the Level IV microprocessor.

REFERENCES

1 R. L. Grob, in R. L. Grob (Editor), *Modern Practice of Chromatography*, Wiley-Interscience, New York, 1977, Ch. 2, p. 64.
2 J. J. van Deemter, F. J. Zuiderweg and A. Klinkenberg, *Chem. Eng. Sci.*, 5 (1956) 271.
3 M. J. E. Golay, in V. J. Coates, H. J. Noebels and I. S. Fagerson (Editors), *Gas Chromatography 1957*, Academic Press, New York, 1958, pp. 1–13.
4 R. L. Grob, in R. L. Grob (Editor), *Modern Practice of Gas Chromatography*, Wiley-Interscience, New York, 1977, Ch. 2, p. 72.
5 W. E. Harris and W. H. Hapgood, *Programmed Temperature Gas Chromatography*, Wiley, New York, 1966, p. v.
6 N. B. Turkeltaub and A. A. Zuchowitsky, *Fortschriftsberichte Gas Chromatographie, 1959*, Akademie Verlag, Berlin, 1961.
7 R. S. Kaiser, *Fresenius' Z. Anal. Chem.*, 189 (1961) 1.
8 L. S. Ettre, *Chromatographia*, 8 (1975) 291.
9 T. A. Rooney and H. J. Hartigan, *J. High Resolut. Chromatogr. Chromatogr. Commun.*, 3 (1980) 416.
10 W. G. Jennings and S. Adam, *Anal. Biochem.*, 69 (1975) 61.
11 J. Krupcik, J. Garaj, G. Guiochon and J. M. Schmitter, *Chromatographia*, 14 (1981) 501.
12 K. Grob, Jr., G. Grob and K. Grob, *J. Chromatogr.*, 156 (1978) 1.
13 K. Grob, Jr. and K. Grob, *J. Chromatogr.*, 207 (1981) 291.
14 L. A. Jones, J. J. Glennon and W. H. Reiss, *J. Chromatogr.*, 595 (1992) 209.
15 L. A. Jones, S. L. Kirby, C. L. Garganta, T. M. Gerig and J. D. Mulik, *Anal. Chem.*, 55 (1983) 1354.
16 L. A. Jones, C. D. Burton, T. A. Dean, T. M. Gerig and J. R. Cook, *Anal. Chem.*, 59 (1987) 1179.
17 H. Purnell, *Gas Chromatography*, Wiley, New York, 1962, pp. 387–388.
18 A. Zlatkis, D. C. Fenimore, L. S. Ettre and J. E. Purcell, *J. Chromatogr.*, 3 (1965) 75.
19 J. Nygren, *J. Chromatogr.*, 142 (1977) 109.
20 L. S. Ettre, I. Mazor and J. Takacs, *Adv. Chromatogr.*, 123 (1969) 271.

21 J. A. Perry, *Introduction to Analytical Gas Chromatography*, Marcel Dekker, New York, 1981, p. 240.
22 J. A. Jönsson, in J. A. Jönsson (Editor), *Chromatographic Theory and Principles*, Marcel Dekker, New York, 1987, p. 59.
23 J. C. Giddings, *Dynamics of Chromatography*, Marcel Dekker, New York, 1965, p. 218.
24 M. Martin and G. Guiochon, *Anal. Chem.*, 54 (1982) 1533.
25 R. Ellis and D. Gulick, *Calculus with Analytical Geometry*, Harcourt Brace Jovanovich, New York, 2nd ed., 1982, p. 203.
26 W. Jennings, *Analytical Gas Chromatography*, Academic Press, New York, 1987, p. 84.